Proceedings of the
International Conference on Mechanical Engineering and Renewable Energy 2011
(ICMERE2011) 22- 24 December 2011, Chittagong, Bangladesh

ICMERE2011-PI-148

Thermal Analyses of Nano and Micro Satellites on Sun-synchronous Orbit by One Nodal Analysis Method

Tsuyoshi Totani, **Hiroto Ogawa**, **Ryota Inoue**, **Masashi Wakita and Harunori Nagata**

Hokkaido University, Kita 13 Nishi 8, Kita-ku, Sapporo, Hokkaido 060-8628, Japan
tota@eng.hokudai.ac.jp*, ogwhrt@ec.hokudai.ac.jp, ryota_inoue@ec.hokudai.ac.jp,
m-wakita@eng.hokudai.ac.jp, nagata@eng.hokudai.ac.jp*

Abstract- *The thermal analyses of nano and micro cubic satellites pointing to the Earth on sun-synchronous and circular orbits have been carried out using one nodal analysis. The altitudes of the orbits are from 300 km to 1000 km. The local time of descending node of the orbits is from 6 to 12. The combination of the solar absorptivity and the infrared emissivity on the surface of the satellite in which the satellite satisfies the allowable temperature range, from 0 to 40 degree Celsius, has been clarified on each of the above orbits. As the heat capacity over one surface area of the satellite is larger, the choice of the combination of the solar absorptivity and the infrared emissivity increases. The number of combination in the case of the orbits without the shadow region is much larger than with the shadow region. The number of the combination in the orbits without the shadow region increases with the higher altitude and the larger projected area with respect to the sun. The number of the combination in the orbit with the shadow region increases with the higher altitude, the larger projected area and the smaller angle of the shadow region.*

Keywords: Thermal Design, Nano Satellite, Micro Satellite, Sun-synchronous Orbit, One Nodal Analysis

1. INTRODUCTION

The heat capacity is defined as the energy required to rise the temperature of 1 K and increases with the cube of the length of satellite. The heat capacity of the nano and micro satellites is small. The temperature change of the nano and micro satellites is larger than that of general satellites with respect to amount of heat. The nano and micro satellites do not have enough electrical power to control the temperature actively using a heater, a heat pipe and a thermal louver that is used by general satellites. It is difficult to control the temperature of a nano and micro satellite within the allowable temperature range of the components in the satellite. The thermal design of nano and micro satellites has been carried out specializing in each of nano and micro satellites. One of the advantages of nano and micro satellites is the shortage of the period of fabrication. It is essential to establish the thermal design guide for a nano and micro satellite in order to shorten the period of thermal design of a nano and micro satellite. In this paper, the thermal analyses of micro and nano satellites pointing to the Earth on sun-synchronous and circular orbits have been carried out using one nodal analysis method for the purpose of establishing the thermal design guide for a nano and micro satellite.

2. METHOD OF ANALYSIS

2.1 Satellite

Table 1 shows the shape, the orbit and the attitude of satellites analyzed in this paper. Most of the missions of nano and micro satellites are observation of the Earth. Earth observation satellites fly on sun-synchronous orbits. The cameras and sensors for earth observations are mounted on a earth-pointing surface of satellites. The size, the mass and the heat capacity of the satellites analyzed in this paper are shown in Table 2. These values of the size and the mass are set by reference to the previously realized satellites [1-4]. There are little data of the specific heat of satellites. The specific heat of three satellites in Table 1 is set to 688 J/(kg K) in such a way that the temperature of satellites change more easily than the realized satellites. This value corresponds to 80 % of the specific heat of aluminum alloy A7050-T7451, 860 J/(kg K) [5].

Table 1. Shape, orbit, attitude and setting method of solar panel of satellites analyzed in this paper.

Shape	Cube
Orbit	Sun-synchronous and circular orbit
Attitude	Earth-pointing
Setting method of solar panel	Body-mounted
Allowable temperature range	0 ～40 degree Celsius

Table 2. Size, mass, heat capacity of satellites.

Model	A	B	C
Size l^3 [m^3]	0.1×0.1×0.1	0.3×0.3×0.3	0.5×0.5×0.5
Mass m [kg]	1	25	50
Heat capacity mc [J/K]	688	17200	34400

2.2 Orbit

Table 3 shows the altitude and the local time at descending node (LTDN) of sun-synchronous orbits analyzed in this paper. The local time at descending node of 12 means that the sun, the orbit of the satellite and the center of gravity of the Earth lie in a same plane. The local time at descending node of 6 means that the sun vector is perpendicular to the orbital plane. The inclination of sun-synchronous and circular orbits is calculated from the following equation [6],

$$0.9856 = -2.06474 \times 10^{14} \frac{\cos i}{(R_e + H)^{3.5}} \quad . \tag{1}$$

The left hand side of Eq.(1) is the rotation angle (degrees) per a mean solar day of the Earth around the sun. The right hand side in Eq.(1) means the regression of nodes of sun-synchronous and circular orbit around the Earth. The inclination corresponding to each altitude is shown in Table 4.

Table 3. Analysis condition of orbit.

Altitude H [km]	300, 500, 700, 1000
Local time at descending node (LTDN)	6, 7, 8, 9, 10, 11, 12

Table 4. Inclination of sun-synchronous orbit.

Altitude H [km]	300	500	700	1000
Inclination i [deg.]	96.67	97.40	98.19	99.48

2.3 Energy Equation

A schematic of input heat to a satellite and output heat from a satellite is shown in Fig.1. The direct radiation from the sun, the albedo and the infrared radiation form the Earth are taken account in this study as the input heat to a satellite. The output heat from a satellite is the infrared radiation. The temperature change per unit time of a satellite in the sun and in the shade is shown in Eq.(2) and Eq.(3), respectively.

$$G_s A_p \alpha + q_{IR}(F_{ns-e} l^2 + 4F_{ps-e} l^2)\varepsilon + G_s a (F_{ns-e} l^2 + 4F_{ps-e} l^2)\alpha \cos\theta_s - \varepsilon\, 6l^2 \sigma T^4 = mc \frac{dT}{dt} \tag{2}$$

$$q_{IR}(F_{ns-e} l^2 + 4F_{ps-e} l^2)\varepsilon - \varepsilon\, 6l^2 \sigma T^4 = mc \frac{dT}{dt} \tag{3}$$

The first term of the left hand side in Eq.(2) means the energy of direct solar radiation which the satellite absorbs. The projected area is calculated by the method of Totani et al [7]. The second term of the left hand side in Eq.(2) indicates the energy of infrared radiation emitted from the earth's surface which the satellite absorbs. The third term of the left hand side in Eq.(2) is the energy of albedo which the satellite absorbs. The Bannister approach [8] is used in the term of the energy

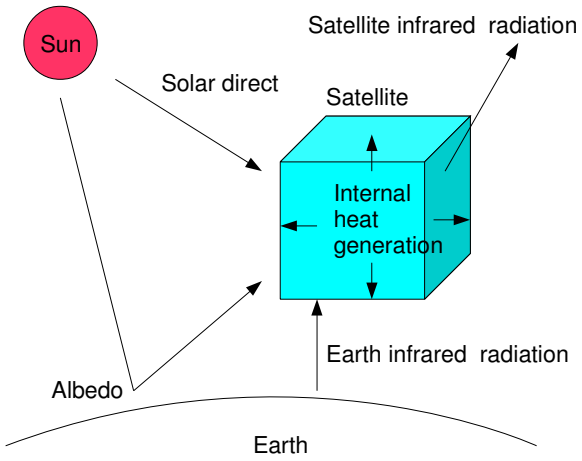

Fig. 1. Schematic of input heat to satellite and output heat from satellite.

of albedo. The fourth term of the left hand side in Eq.(2) means the radiative energy emitted from the whole surfaces of a satellite. It is known that F_{ns-e} and F_{ps-e} are shown in Eq.(4) and Eq.(5) [9].

$$F_{ns-e} = \left(\frac{R_e}{R_e + H} \right)^2 . \tag{4}$$

$$F_{ps-e} = \frac{1}{\pi} \left(\tan^{-1} \frac{1}{\sqrt{\left(\frac{R_e + H}{R_e} \right)^2 - 1}} - \frac{\sqrt{\left(\frac{R_e + H}{R_e} \right)^2 - 1}}{\left(\frac{R_e + H}{R_e} \right)^2} \right) . \tag{5}$$

2.4 Worst Hot Case and Worst Cold Case

The worst hot case and the worst cold case are shown in Table 5. A satellite is designed such a way that the design temperature becomes within the allowable temperature limits of components in the satellite. A satellite is separated at the exit of the shadow region in the worst hot case and at the entrance of the shadow region in the worst cold case.

Table 5. Worst hot case and worst cold case.

	Worst hot case	Worst cold case
Earth IR radiation q_{IR} [W/m^2]	258	140
Solar constant G_s [W/m^2]	1399	1309
Albedo factor a	0.60	0.15
Initial temperature [degree Celsius]	25	10
Initial position	τ_{out}	τ_{in}

2.5 Calculation procedure

The flow chart of the calculation procedure is shown in Fig.2. The grids of the calculation divide an orbit into 8000 parts in such a way that grids locate on the entrance and the exit of the region of eclipse. α and ε are set at 0.01 intervals, respectively. The terminal condition of the calculation of 600 π rad. have no important meaning. This value was adopted to calculate until the temperature change during one trip of an orbit become stable.

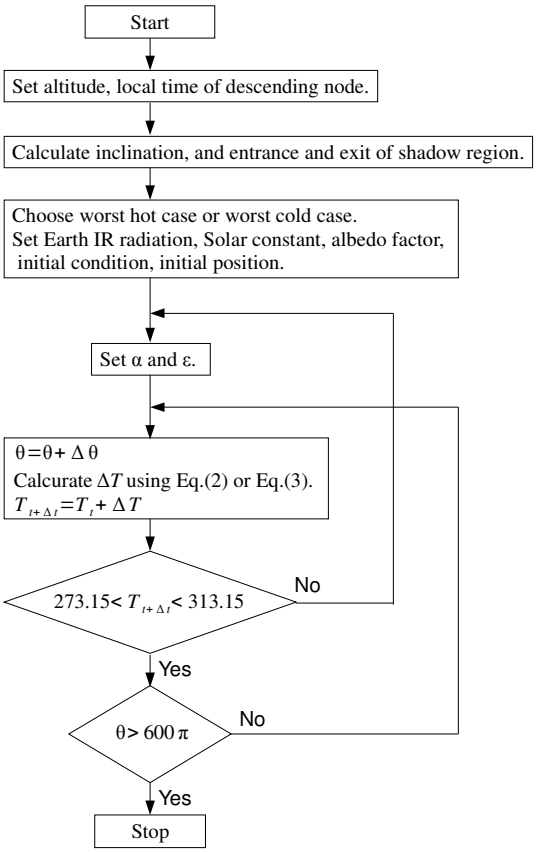

Fig. 2. Flow chart of calculation procedure.

3. RESULTS AND DISCUSSIONS

Figure 3 shows the combination of α and ε in which the temperature of satellite model A, B and C satisfies the allowable temperature range in both the worst hot case and the worst cold case on the orbit with the altitude of 500 km and the local time of descending node of 11. This figure indicates that the combination of α smaller than 0.3 and ε smaller than 0.2 satisfies the allowable temperature range in satellite model A, the combination of α smaller than 0.7 and ε smaller than 0.5 satisfies the allowable temperature range in satellite model B and the combination of α smaller than 0.5 and ε smaller than 0.35 satisfies the allowable temperature range in satellite model C. Figure 3 tells that the number of the combination of α and ε satisfying the allowable temperature range increases not in the order of A, B, C, but in the order of A, C, B. As shown in Table 2, the heat capacity of satellite model A, B and C increases in the order of A, B and C. Figure 3 means that the combination of α and ε satisfying the allowable temperature range are independent from the heat capacity of satellites. Substituting Eq.(23) into Eq.(2) and dividing both sides by l^2, the following equations is obtained.

$$G_s A_{pi}\alpha + q_{IR}(F_{ns-e}+4F_{ps-e})\varepsilon + G_s a(F_{ns-e}+4F_{ps-e})\alpha\cos\theta_s - \varepsilon\, 6\sigma T^4 = \frac{mc}{l^2}\frac{dT}{dt} \quad (6)$$

Dividing both sides of Eq.(3) by l^2, the following equation is obtained.

$$q_{IR}(F_{ns-e}+4F_{ps-e})\varepsilon - \varepsilon\, 6\sigma T^4 = \frac{mc}{l^2}\frac{dT}{dt} \quad (7)$$

These equations tell that the temperature change with respect to time depends on the parameter of mc/l^2. The value of the parameter of mc/l^2 of satellite model A, B and C are shown in Table 6. The magnitude of parameter mc/l^2 of satellite model A, B, C increase in the order of A, C, B. This order corresponds to the order of the increase of the number of the combination of α and ε. l^2 is the area of a surface of a satellite. The amount of the radiative heat output from a satellite and the amount of the radiative heat input to a satellite depend on the area of a surface of a satellite. The smaller the area of a surface of a satellite is, the smaller the temperature change is. The larger heat capacity is, the smaller the temperature change is. As parameter mc/l^2 is larger, the temperature change is smaller. It is difficult to mount the active thermal control system in a nano and micro satellite because of the limitation of power resources and the smallness of space. Parameter mc/l^2 is effective to evaluate the easiness of the thermal design of nano and micro satellites.

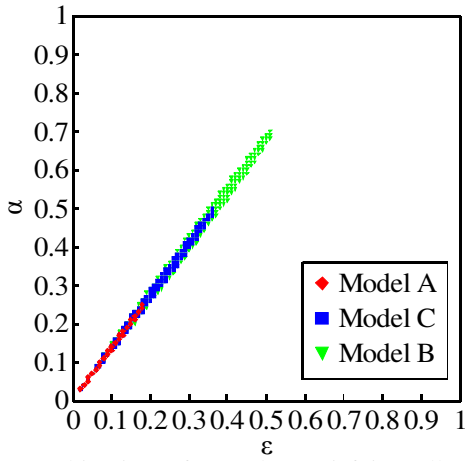

Fig. 3. Combination of α and ε satisfying allowable temperature range in worst hot case and worst cold case.

Table 6. Parameter mc/l^2 of satellite model A, B and C.

Model	A	B	C
mc/l^2 [J/K/m^2]	68800	191111	137600

It is difficult to increase the mass of a nano and micro satellite in order to increase the choice of the optical properties on the surface of the satellite because the weight of nano and micro satellites are restricted in many cases of the piggy back launch. Figure 4 shows the combination of α and ε in which the temperature of satellite model B with the specific heat of 688, 1000 and 2000 [J/kg/K] satisfies the allowable temperature range in both the worst hot case and the worst cold case on the orbit with the altitude of 500 km and the local time of descending node of 11. The specific heat of 2000 [J/kg/K] corresponds to about a half of the specific heat of water. The combination of α and ε increases as the specific heat is larger in Fig.4. This means that it is effective to increase the specific heat of a whole satellite in order to increase the choice of optical properties on the surface of a satellite. The solar array is mounted on the surface of nano and micro satellites without using the deployment structure. Many of nano and micro satellites

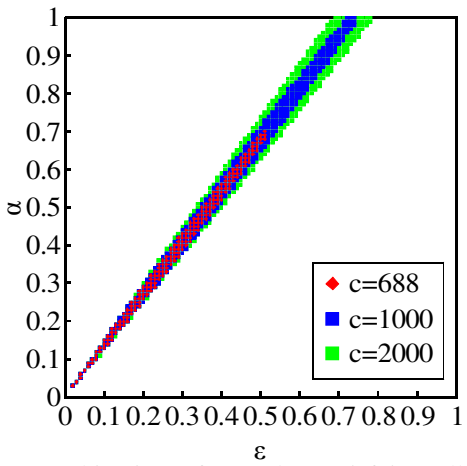

Fig. 4. Combination of α and ε satisfying allowable temperature range in worst hot case and worst cold case.

do not have enough power resources to control the temperature actively. Figure 4 suggests that heat storage materials fit well in order to increase the heat capacity of nano and micro satellites.

Table 7, Table 8 and Table 9 show the number of the combination of α and ε in which the temperature of satellite model A, B and C, respectively, satisfy the allowable temperature range under both the worst hot condition and the worst cold condition. The colored cells in these tables indicate the orbit without the shadow region. The number of the combination of α and ε in the orbit without the shadow region is much larger than that in the orbit with the shadow region.

The results obtained in the orbits with the shadow region are discussed. In the case of different altitudes and a same local time of descending node, the number of the combination of α and ε becomes larger as the altitude becomes higher. Not only the configuration factor, but also the angle of shadow region is smaller as the altitude is higher. The angles of shadow region are shown in Table 10. The decrease of the angle of shadow region leads to the increase of the angle of sunshine region. The increase of the angle of sunshine region leads to the increase of the energy of direct solar radiation and albedo absorbed by a satellite. These increase of energy cause the increase of temperature of the satellite. The decrease of the angle of shadow region has the opposite effect from the decrease of the configuration factor. The temperature histories of satellite model B circling the Earth during 100 rounds on the orbit with the altitude of 500 km and 1000 km and the local time of descending node of 11 under the worst hot case and the worst cold case are shown in Fig.5. α and ε is 0.29 and 0.20, respectively. The temperature on the orbit with the altitude of 1000 km is lower than the altitude of 500 km under the worst hot case, while the temperature on the orbit with the altitude of 1000 km is higher than the temperature on the orbit with the altitude of 500 km under the worst cold case. The effect of the decrease of the configuration factor is stronger than the effect of the decrease of the angle of shadow region under the worst hot case, while the effect of the decrease of the angle of shadow region is stronger than the effect of the decrease of the configuration factor under the worst cold case. This suggests that the increase of the number of the combination of α and ε with the higher altitude is caused by the above reason.

Table 7. Number of combination of α and ε satisfying allowable temperature range under worst hot case and worst cold case in model A.

LTDN	Altitude H [km]	300	500	700	1000
12		6	19	28	35
11		16	26	33	41
10		24	32	41	48
9		37	52	62	82
8		64	96	153	528
7		183	1583	1629	1664
6		1611	1643	1663	1680

Table 8. Number of combination of α and ε satisfying allowable temperature range under worst hot case and worst cold case in model B.

LTDN	Altitude H [km]	300	500	700	1000
12		72	142	205	279
11		125	201	254	313
10		194	269	325	392
9		295	392	484	626
8		507	753	1061	1476
7		1056	1735	1762	1782
6		1739	1754	1757	1764

Table 9. Number of combination of α and ε satisfying allowable temperature range under worst hot case and worst cold case in model C.

LTDN	Altitude H [km]	300	500	700	1000
12		33	76	103	142
11		65	103	133	164
10		100	133	169	201
9		155	204	249	330
8		262	393	611	1352
7		748	1701	1731	1760
6		1711	1729	1733	1747

In the case of a same altitude and different local time of descending node, the number of the combination of α and ε increases as the local time of descending node becomes smaller. The angle of shadow region and the projected area with respect to the sun depends on the local time of descending node. The angle of shadow

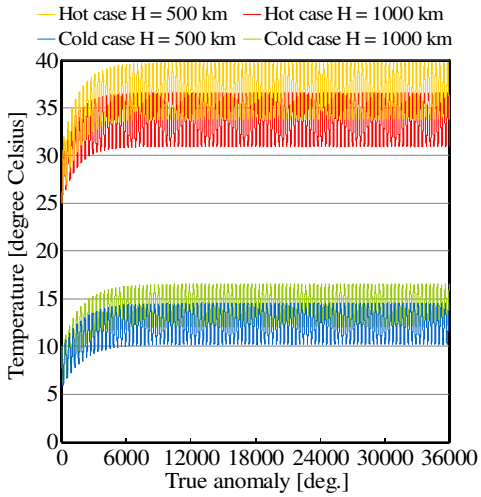

Fig. 5. Temperature histories of satellite model B circling on orbit with altitude of 500 km and 1000 km and local time of descending node of 11 under worst hot case and worst cold case.

region is smaller as the local time of descending node is smaller in the case of a same altitude as shown in Table 10. The projected area with respect to the sun is shown in Fig. 6. As shown in this figure, the projected area with respect to the sun is the largest at the local time descending time of 9 or 10. The number of the combination of α and ε increases as the local time of descending node becomes smaller and does not have a peak at the local time descending time of 9 or 10. It follows that the increase of the number of the combination of α and ε is caused by the decrease of the angle of shadow region. The decrease of the angle of shadow region leads to the increase of the angle of sunshine region. The increase of the angle of sunshine region leads to the increase of the energy of direct solar radiation and albedo absorbed by a satellite. These increase of energy cause the increase of temperature of the satellite. The number of the combination of α and ε does not increase if the temperature rise under worst hot case is same with that under worst cold case because the number of the combination of α and ε in which the temperature of a satellite enters in the allowable temperature range under the worst cold case is same with the number of the combination of α and ε in which the temperature of a satellite departs from the allowable temperature range under the worst hot case. The relative increment of the energy of direct solar radiation to the energy of infrared radiation and of the albedo absorbed by the satellite under the worst cold case is larger than that under the worst hot case because Earth IR radiation under the worst cold case is 25% of that under the worst hot case and the albedo factor under the worst cold case is 54% of that under the worst hot case, while the solar constant under the worst cold case is 94% of that under the worst hot case.

The results obtained in the orbit without the shadow region are discussed. The number of the combination of α and ε in the orbit with the local time of descending node of 7 is larger than 6 in comparison with a same altitude. The number of the combination of α and ε is larger as the altitude is higher in the case of a same local

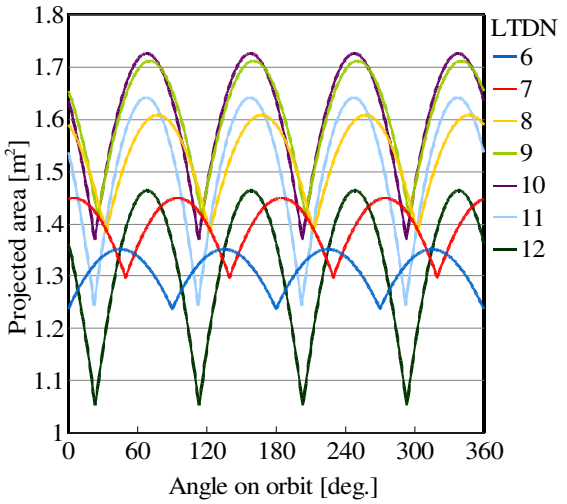

Fig. 6. Projected area with respect to sun in case of altitude of 500 km.

time of descending node. In the case of a same altitude and different local time of descending node, the only projected area with respect to the sun is different as shown in Eq.(2). The projected area with respect to the sun is shown in Fig. 6. The projected area with respect to the sun in the case of the local time of descending node of 7 is larger than 6. This means that a satellite absorbs the more energy of direct solar radiation and the temperature of the satellite becomes higher. The relative increment of the energy of direct solar radiation to the energy of infrared radiation and of the albedo absorbed by the satellite under the worst cold case is larger than that under the worst hot case because Earth IR radiation under the worst cold case is 25% of that under the worst hot case and the albedo factor under the worst cold case is 54% of that under the worst hot case, while the solar constant under the worst cold case is 94% of that under the worst hot case. This leads that the rise of temperature relate to the increase of the projected area with respect to the sun under the worst cold case is larger than under the worst hot case. It follows that the number of the combination of α and ε achieving that the temperature of a satellite enters in the allowable temperature range under the worst cold case is larger than the number of the combination of α and ε causing that the temperature of a satellite departs from the allowable temperature range under the worst hot case, by the rise of the temperature of a satellite relate to the increase of the projected area with respect to the sun. In the case of a different altitude and a same local time of descending node, the configuration factor corresponding the altitude are different as shown in Eq. (4) and (5). The configuration factor becomes smaller with the higher altitude. This means that the energy of infrared radiation and the energy of albedo absorbed by a satellite are smaller with the higher altitude and the temperature of the satellite decreases. The relative decrement of the energy of infrared radiation and the energy of albedo to the energy of direct solar radiation absorbed by the satellite under the worst hot case is larger than that under the worst cold case as described above. It follows that the number of the combination of α and ε achieving that the temperature of a satellite enters in the allowable temperature range

under the worst hot case is larger than the number of the combination of α and ε causing that the temperature of a satellite departs from the allowable temperature range under the worst cold case, by the decrease of the temperature of a satellite relate to the increase of the altitude.

4. CONCLUSIONS

The thermal design of micro and nano satellites pointing to the Earth on sun-synchronous and circular orbits has been carried out. The mass of the satellites analyzed in this paper is 1 kg, 25 kg and 50 kg. The shape of the satellites is cube. The specific heat of the satellites is set 688 J/(kg K) that corresponds to 80 % of the specific heat of aluminum alloy A7050-T7451. The altitudes of the orbits are 300 km, 500 km, 700 km and 1000 km. The local time of descending node of the orbit is 6, 7, 8, 9, 10, 11 and 12. The allowable temperature range of the satellites is from 0 to 40 degree Celsius. The combination of the solar absorptivity and the infrared emissivity on the surface of the satellite in which the satellite satisfies the allowable temperature range has been clarified on each of the above orbits. This work contributes to the thermal design of micro and nano satellites pointing to the Earth on sun-synchronous and circular orbits. The number of the combination of the solar absorptivity and the infrared emissivity does not depend on the heat capacity of satellites but depends on the parameter of the heat capacity of the satellite over one surface area of the satellite. As the parameter is larger, the choice of the combination of the solar absorptivity and the infrared emissivity increases. The number of the combination of the solar absorptivity and the infrared emissivity in the case of the orbit without the shadow region is much larger than with the shadow region. The number of the combination of the solar absorptivity and the infrared emissivity in the case of the orbit without the shadow region increases with the higher altitude and the larger projected area with respect to the sun. The number of the combination of the solar absorptivity and the infrared emissivity in the case of the orbit with the shadow region increases with the higher altitude, the larger projected area with respect to the sun and the smaller angle of the shadow region.

5. ACKOWLEDGEMENT

This research is granted by the Japan Society for the Promotion of Science (JSPS) through the "Funding Program for World-Leading Innovative R&D on Science and Technology (FIRST Program)," initiated by the Council for Science and Technology Policy (CSTP).

6. REFERENCES

[1] Funase, R., Takei, E. et al.: Technology Demonstration on University of Tokyo's Pico-satellite "XI-V" and Its Effective Operation Result using Ground Station Network, *Acta Astronaoutica*, **61** (2007), pp.707-711.

[2] Totani, T., II, H, et al.: Preliminary Thermal Design of UNITEC-1, *Trans. JSASS Aerospace Tech. Japan*, **8**, ists27 (2010), pp. Pf_1-Pf_6.

[3] Hayashi, T., Okamoto, Y., et al.: Whale Ecology Observation Satellite System, *IEIC Technical Report (Institute of Electronics, Information and Communication Engineers)*, **103**, 531(SANE2003 85-92) (2003), pp.19-25

[4] Yoshida, K., Takahashi, Y., et al.: SPRITE-SAT: a Micro Satellite for Scientific Observation of Transient Luminous Events and Terrestrial Gamma-Ray Flashes, *Trans. JSASS Aerospace Tech. Japan*, **8**, ists27 (2010), pp. Tm_7-Tm_12.

[5] Japan Aluminum Association: *Characteristics Database of Aluminum Materials*, http://metal.matdb.jp/JAA-DB/ (in Japanese).

[6] Brown, C. D.: *Spacecraft Mission Design, 2nd ed.*, AIAA, Reston, 1998, pp.87-89.

[7] Totani, T., Ogawa, H. et al.: Thermal Design of Nano and Micro Satellites on Sun-synchronous Orbit, *Proceedings of 28th International Symposium on Space Technology and Science*, 2011-f-34, 2011.

[8] Bannister, J. C.: *Radiation Geometry Factor between the Earth and a Satellite*, NASA TND-2750, 1965.

[9] Siegel, R. and Howell, J. R.: *Thermal Radiation Heat Transfer, 2nd ed.*, Hemisphere Publishing Corporation, New York, 1981, p.829.

7. NOMENCLATURE

Symbol	Meaning	Unit
a	albedo factor	-
A_p	projected area	m^2
A_{pi}	non-dimensional projected area	-
c	specific heat, J/(kg·K)	m
F	configuration factor	-
G_s	solar constant	W/m^2
H	altitude	km
i	inclination	degree
l	length of side of satellite	m
m	mass	kg
q_{IR}	earth IR radiation	W/m^2
R_e	radius of Earth, 6378.14	km
t	time	s
T	temperature	K
α	solar absorptivity	-
ε	infrared emissivity	-
θ	zenith angle	rad
s		
σ	Stefan-Boltzmann contact	$W/(m^2K^4)$
π	circular constant	-
τ	shadow region	-

Subscripts

Symbol	Meaning
in	entrance of shadow region
ns-e	from the earth pointing surface of a satellite to the Earth
out	exit of shadow region
ps-e	from the surface parallel to the position vector of a satellite to the Earth